

Incoherent diffractive J/Ψ production in high-energy nuclear deep-inelastic scatteringT. Lappi^{1,2} and H. Mäntysaari¹¹*Department of Physics, P.O. Box 35, FI-40014 University of Jyväskylä, Finland*²*Helsinki Institute of Physics, P.O. Box 64, FI-00014 University of Helsinki, Finland*

(Received 18 November 2010; revised manuscript received 13 May 2011; published 14 June 2011)

We compute cross sections for incoherent diffractive J/Ψ production in lepton-nucleus deep-inelastic scattering (DIS). The cross section is proportional to A in the dilute limit and to $A^{1/3}$ in the black disk limit, with a large nuclear suppression due to saturation effects. The t dependence of the cross section, if it can be measured accurately enough, is sensitive to the impact parameter profile of the gluons in the nucleus and their fluctuations, a quantity that determines the initial conditions of a relativistic heavy-ion collision. The nuclear suppression in incoherent diffraction shows how the transverse spatial distribution of the gluons in the nucleus gradually becomes smoother at high energy. Since the values of the momentum transfer $|t|$ involved are relatively large, this process should be easier to measure in future nuclear DIS experiments than coherent diffraction.

DOI: [10.1103/PhysRevC.83.065202](https://doi.org/10.1103/PhysRevC.83.065202)

PACS number(s): 13.60.Hb, 24.85.+p

I. INTRODUCTION

Strongly interacting systems in the high-energy (or small x) limit are very nonlinear systems in spite of the smallness of the coupling constant α_s . This is due to the large phase space available for semihard gluon radiation that increases the occupation numbers of gluonic modes in the hadron or nucleus wave function. Thus, high-energy scattering has to be understood in terms of gluon recombination and saturation that enforce the unitarity requirements of the S matrix. This happens naturally in the color glass condensate (CGC) effective theory of the high-energy wave function. In the context of deep-inelastic scattering (DIS) the CGC leads to the dipole picture that naturally gives a consistent description of both inclusive and diffractive scattering. The nonlinearities in high-energy scattering are enhanced when the target is changed from a proton to a heavy nucleus. Thus there is a great opportunity to understand them by studying nuclear DIS in new collider experiments, such as the EIC [1] or the LHeC [2]. The particular process we discuss in this paper is diffractive DIS on nuclei.

In the Good-Walker [3] picture of diffraction one needs to identify the states that diagonalize the imaginary part of the T matrix. In the case of nuclear DIS at high energy these states are the ones with the virtual photon fluctuating into a dipole of a fixed size r and with the nucleons in the nucleus at fixed transverse positions b_i . In coherent diffraction the nucleus is required to stay intact, which corresponds to performing the average over the nuclear wave function at the level of the scattering amplitude. Averaging the cross section, instead of the amplitude, over the nucleon positions allows for the nucleus to break up, giving the sum of incoherent and coherent cross sections, i.e., the quasielastic cross section. For a more formal discussion of this we point the reader to, e.g., Ref. [4]. The t dependence of the incoherent cross section therefore directly probes the fluctuations and correlations in the nuclear wave function, which have turned out to be a crucial ingredient in understanding the initial conditions in heavy-ion collisions [5].

The average gluon density probed in the coherent process is very smooth, meaning that the cross section is dominated

by small values of momentum transfer to the nucleus, $t \sim -1/R_A^2$. Measuring such a small momentum transfer accurately is very challenging. At momentum scales corresponding to the nucleon size $t \sim -1/R_p^2$ the diffractive cross section is almost purely incoherent. The larger momentum transfer should also be easier to reconstruct experimentally, even without measuring the transverse momentum of the nuclear remnants, by accurately reconstructing the outgoing electron and J/Ψ momenta and using momentum conservation. By taking these processes into account in the detector design one should be capable of measuring diffractive events at a higher accuracy than was done at HERA. In the dilute limit (for small dipoles) there is no multiple scattering, and the incoherent cross section is given by A times the corresponding one for protons. The deviation of the t slope from the proton measures the transverse size of the fluctuating areas in the nucleus.

In the black disk limit the nucleus is smooth not only on average but also event by event, leading to a strong suppression of the incoherent cross section. Incoherent diffraction gets contributions from the edge of the nucleus, making the cross section asymptotically behave as $\sim A^{1/3}$ in contrast to $\sim A$ in the dilute limit. The suppression in the normalization relative to the proton is a measure of the approach to the unitarity limit in the dipole cross section. It is a clear signal of how individual nucleons have lost their identity in the sense that they cannot be resolved by the virtual photon. It is precisely this suppression that we are proposing to use to quantitatively access saturation effects in the nuclear wave function. The purpose of this paper is to provide a realistic estimate of the nuclear suppression in diffractive cross sections in a regime that could be measured in future nuclear DIS experiments.

Nuclear DIS data from fixed target experiments, in particular E665 [6] and NMC [7], have already been much discussed in the literature as demonstrations of *color transparency* (see, e.g., Refs. [8–12]). The form of nuclear modification to the incoherent diffraction in terms of the dipole cross section that we have rederived is not new (see, e.g., Refs. [11,13]). So far, however, less attention has been paid to inelastic diffraction in future DIS experiments. The production cross sections

have not been calculated using the same CGC-inspired cross sections that have been used successfully to confront HERA data, as we intend to do here. In this work we concentrate on the J/Ψ because its small size means that the interaction of the dipole with the target is calculable in weak coupling even at small Q^2 .

The importance of diffraction in understanding gluon saturation has been discussed and our basic setup motivated in Ref. [14]. Nuclear modifications to the diffractive structure functions, integrated over the momentum transfer t , were computed in Ref. [15]. Vector-meson production at future DIS experiments was recently discussed from a more experimental point of view in Ref. [4], and coherent production cross sections (integrated over t) were calculated in Ref. [16]. An interesting discussion on coherent and incoherent diffraction and gluon saturation in the nucleus can be found in Ref. [17]. In this study we want to take a step beyond the discussion of inclusive diffraction in Refs. [14,15] to understand the t dependence in more detail.

II. DIPOLE CROSS SECTIONS

There are many dipole cross-section parametrizations available in the literature, and we have taken for this study two representative samples. One is the IIM [18] dipole cross section, which is a parametrization including the most important features of BK [19] evolution. The detailed expression for the dipole cross section can be found in Ref. [18]; we use here the values of the parameters from the newer fit to HERA data including charm [20] that was also used to compute diffractive structure functions in Ref. [21]. We also want to compare our results to a parametrization with an eikonalized DGLAP-evolved gluon distribution. For this purpose we will use an approximation of the IPSat dipole cross section [22,23].

To extend the dipole cross section from protons to nuclei we will take the independent scattering approximation that is usually used in Glauber theory and write the S matrix as

$$S_A(\mathbf{r}_T, \mathbf{b}_T, x) = \prod_{i=1}^A S_p(\mathbf{r}_T, \mathbf{b}_T - \mathbf{b}_{T_i}, x). \quad (1)$$

Here we conventionally parametrize the energy dependence of the scattering amplitude with x , the Bjorken variable of the DIS event.¹ The variables \mathbf{b}_{T_i} in Eq. (1) are the nucleon coordinates that we will discuss in Sec. III. This independent scattering assumption is natural in IPSat-like parametrizations or the MV [24] model, where, denoting $r = |\mathbf{r}_T|$, $S(\mathbf{r}_T) \sim e^{-r^2 Q_s^2/4}$ with a saturation scale Q_s^2 proportional to the nuclear thickness $T_A(b)$. High-energy evolution, however, introduces an anomalous dimension that leads, in the nuclear case, to what could be called leading twist shadowing. With an anomalous dimension $S \sim e^{-(Q_s r)^{2\gamma}}$ with $\gamma \neq 1$, a proportionality $Q_s^2 \sim T_A(b)$ is

¹Note that, strictly speaking, the relation between x and the energy of the dipole-target scattering depends on Q^2 , not only r . Using x here is justified in a high-energy approximation where the energy of the dipole in the target rest frame is approximately the same as that of the virtual photon.

not equivalent to Eq. (1). A solution to this problem (see also the more detailed discussion in Ref. [15]) would require a realistic impact-parameter-dependent solution to the BK equation which, we feel fair to say, is not yet available. We point the reader to, e.g., Ref. [25] for a discussion of the difficulties. These are related to the long-distance Coulomb tails that, physically, are regulated at the confinement length scale that is not enforced in a first-principles weak-coupling calculation. The effect of BK evolution is important for the CGC description of the forward suppression of particle production in dAu collisions at RHIC (for a review, see Ref. [26]). In our case the difficulty is greater since we are interested not only in the relatively smooth average gluon density but also its variations at smaller length scales of the order of the proton radius. We thus leave the modifications of Eq. (1) due to the effects of evolution to a future study.

The IIM parametrization assumes, either explicitly or implicitly, a factorizable \mathbf{b}_T dependence

$$\begin{aligned} \frac{d\sigma_{\text{dip}}^p(\mathbf{b}_T, \mathbf{r}_T, x)}{d^2\mathbf{b}_T} &= 2[1 - S_p(\mathbf{r}_T, \mathbf{b}_T, x)] \\ &= 2T_p(\mathbf{b}_T)\mathcal{N}(r, x), \end{aligned} \quad (2)$$

We take, following Ref. [21], a Gaussian profile $T_p(\mathbf{b}_T) = \exp(-b^2/2B_p)$ with $B_p = 5.59 \text{ GeV}^{-2}$ (see Sec. IV for a discussion of this largish numerical value).

In the IPSat model the impact parameter dependence is included in the saturation scale as

$$\frac{d\sigma_{\text{dip}}^p(\mathbf{b}_T, \mathbf{r}_T, x)}{d^2\mathbf{b}_T} = 2\{1 - \exp[-r^2 F(x, r)T_p(\mathbf{b}_T)]\}. \quad (3)$$

Here $T_p(\mathbf{b}_T) = \exp(-b^2/2B_p)$ is the impact parameter profile function in the proton with $B_p = 4.0 \text{ GeV}^2$, and F is proportional to the DGLAP evolved gluon distribution [27],

$$F(x, r^2) = \frac{1}{2\pi B_p} \frac{\pi^2}{2N_c} \alpha_s \left(\mu_0^2 + \frac{C}{r^2} \right) x g \left(x, \mu_0^2 + \frac{C}{r^2} \right), \quad (4)$$

with C chosen as 4 and $\mu_0^2 = 1.17 \text{ GeV}^2$ resulting from the fit [23]. The proton dipole cross sections used are plotted in Fig. 1 for $x = 0.0001$.

We would generally prefer the unfactorized b dependence of Eq. (3) to the factorized one in Eq. (2) because it allows for the correct unitarity limit of the scattering amplitude at all impact parameters (see the discussion in Ref. [15]). However, there seems to be no clear difference between the two in terms of the quality of the description of HERA data, and for the sake of computational simplicity we will in this work limit ourselves to the factorized dependence and approximate the IPSat dipole cross section by

$$\frac{d\sigma_{\text{dip}}^p(\mathbf{b}_T, \mathbf{r}_T, x)}{d^2\mathbf{b}_T} \approx 2T_p(\mathbf{b}_T)\{1 - \exp[-r^2 F(x, r)]\} \quad (5)$$

using the same $F(x, r)$ defined in Eq. (4). This approximation brings the IPSat parametrization to the form (2) with $\mathcal{N}(r, x) = \{1 - \exp[-r^2 F(x, r)]\}$; in fact, this is the form used already in Ref. [27]; we, however, use the gluon distribution from the IPSat fit [23] for convenience. Improving this description goes

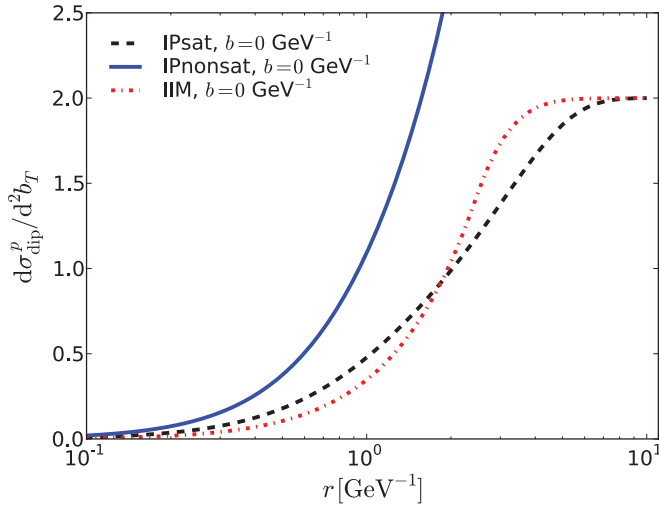


FIG. 1. (Color online) The r dependence of the different proton dipole cross sections used, at $x = 0.0001$ and $b = 0$. As discussed in Sec. IV, the “IPnonsat” curve is Eq. (5) linearized in $r^2 F(x, r)$.

hand in hand with giving up the approximation of independent scatterings off the nucleons, Eq. (1), and is left for future work. As we shall see in the following, these approximations enable us to write the cross section for incoherent diffraction in a form that is much simpler to evaluate numerically than one with a general b dependence.

III. COMPUTING DIFFRACTIVE CROSS SECTIONS

The cross section for quasielastic vector-meson production in nuclear DIS is

$$\frac{d\sigma^{\gamma^*A \rightarrow VA}}{dt} = \frac{R_g^2(1 + \beta^2)}{16\pi} \langle |\mathcal{A}(x_{\mathbb{P}}, Q^2, \Delta_T)|^2 \rangle_N, \quad (6)$$

with $t = -\Delta_T^2$. The dipole cross section is evaluated at the energy scale corresponding to the rapidity gap between the vector meson and the target $x_{\mathbb{P}}$. To translate this into the photon-target center-of-mass energy W that is often used to present experimental results, note that $x_{\mathbb{P}} = (M_{J/\Psi}^2 + Q^2)/(W^2 + Q^2)$. The factor $1 + \beta^2$ accounts for the real part of the scattering amplitude, and the factor R_g^2 corrects for the skewedness effect, i.e., that the gluons in the target are probed at slightly different x [29]. For these corrections we follow the prescription of Ref. [30], taking them as

$$\beta = \tan \frac{\pi \lambda}{2}, \quad (7)$$

$$R_g = \frac{2^{2\lambda+3}}{\sqrt{\pi}} \frac{\Gamma(\lambda + 5/2)}{\lambda + 4}, \quad (8)$$

with

$$\lambda = \frac{\partial \ln \mathcal{A}_{T,L}^{\gamma^*p \rightarrow J/\Psi p}}{\partial \ln 1/x_{\mathbb{P}}}. \quad (9)$$

These corrections depend, in general, on t , which we take into account in our calculation. For the full IPsat model λ changes by about 5% between $t = 0$ and $-t = 0.5 \text{ GeV}^2$.

For the factorized impact parameter dependence in Eqs. (2) and (5) λ is independent of t . We calculate the correction terms from the energy dependence of the nucleon scattering amplitudes and use the same values for the nucleus at the same $Q^2, x_{\mathbb{P}}$. Since the difference in λ extracted from the nucleus and the nucleon cross sections is small (compared to the value of λ) and R_g and β are in themselves corrections to the cross section, this approximation is justified. In addition this approximation has the advantage that these corrections cancel on the nucleus-nucleon cross-section ratio. The real part and skewedness corrections, especially R_g , are, however, a significant factor in the absolute normalization of the cross section and are necessary for the agreement with HERA data.

The imaginary part of the scattering amplitude is the Fourier transform of the dipole cross section from \mathbf{b}_T to Δ_T contracted with the overlap between the vector-meson and virtual-photon wave functions:

$$\begin{aligned} \mathcal{A}(x_{\mathbb{P}}, Q^2, \Delta_T) &= \int d^2\mathbf{r}_T \int \frac{dz}{4\pi} \int d^2\mathbf{b}_T [\Psi_V^* \Psi](r, Q^2, z) \\ &\times e^{-i\mathbf{b}_T \cdot \Delta_T} \frac{d\sigma_{\text{dip}}}{d^2\mathbf{b}_T}(\mathbf{b}_T, \mathbf{r}_T, x_{\mathbb{P}}), \end{aligned} \quad (10)$$

where we have followed the normalization convention of [23]. For the virtual-photon–vector-meson wave-function overlap we use the “boosted Gaussian” parametrization from Ref. [23]. We have also tested the “gaus-LC” wave function also used in Ref. [23]. Although the “boosted Gaussian” seems preferred by HERA data, the gaus-LC parametrization is also compatible with the data within the experimental errors. The cross sections for the proton differ by factors of the order of 10%. The interaction of the gluon target with the dipole can in general depend also on Δ_T , which introduces terms that couple \mathbf{r}_T , Δ_T , and z in Eq. (10). For the J/Ψ and the range in t considered in this paper Δ_T is sufficiently small compared to the relevant values of $1/r$ that we can neglect this coupling, which simplifies the structure considerably. Lighter vector mesons would require a more general treatment.

The average over the positions of the nucleon in the nucleus is denoted here by

$$\langle \mathcal{O}(\{\mathbf{b}_{Ti}\}) \rangle_N \equiv \int \prod_{i=1}^A [d^2\mathbf{b}_{Ti} T_A(\mathbf{b}_{Ti})] \mathcal{O}(\{\mathbf{b}_{Ti}\}). \quad (11)$$

Here T_A is the Woods-Saxon distribution with nuclear radius $R_A = (1.12A^{1/3} - 0.86A^{-1/3}) \text{ fm}$ and surface thickness $d = 0.54 \text{ fm}$. This expectation value is equivalent to the average over nucleon configurations in a Monte Carlo Glauber calculation. We are assuming that the positions \mathbf{b}_{Ti} are independent, i.e., neglecting nuclear correlations that would be a subject of interest in their own right (see, e.g., [31]). The coherent cross section is obtained by averaging the amplitude before squaring it, $|\langle \mathcal{A} \rangle_N|^2$, and the incoherent one is the variance $\langle |\mathcal{A}|^2 \rangle_N - |\langle \mathcal{A} \rangle_N|^2$ that measures the fluctuations of the gluon density inside the nucleus. Because $\langle \mathcal{A} \rangle_N$ is a very smooth function of \mathbf{b}_T , its Fourier transform vanishes rapidly for $\Delta \gtrsim 1/R_A$. Therefore at large Δ the quasielastic cross section (6) is almost purely incoherent.

The cross section for quasielastic vector-meson production is now expressed in terms of the dipole scattering amplitude as

$$\begin{aligned} \frac{d\sigma^{\gamma^*A \rightarrow V A^*}}{dt} &= \frac{R_g^2(1 + \beta^2)}{16\pi} \int \frac{dz}{4\pi} \frac{dz'}{4\pi} d^2\mathbf{r}_T d^2\mathbf{r}'_T \\ &\times [\Psi_V^* \Psi](r, z, Q) [\Psi_V^* \Psi](r', z', Q) \\ &\times \langle |\mathcal{A}_{q\bar{q}}|^2(x_{\mathbb{P}}, r, r', \mathbf{\Delta}_T) \rangle_N. \end{aligned} \quad (12)$$

We now average the square of the dipole scattering amplitude over the nucleon coordinates using the assumptions of Eqs. (1) and (2) and taking the large A limit. We are additionally assuming that T_A is a smooth function on the distance scale defined by B_p . Averaging the square of the amplitude gives the total quasielastic contribution, but we only keep the terms that contribute at large $|t| \gg 1/R_A^2$, which leaves us with the expression

$$\begin{aligned} |\mathcal{A}_{q\bar{q}}|^2(x_{\mathbb{P}}, r, r', \mathbf{\Delta}_T) &= 16\pi B_p \int d^2\mathbf{b}_T \sum_{n=1}^A \frac{1}{n} \binom{A}{n} e^{-B_p \Delta_T^2/n} \\ &\times e^{-2\pi B_p A T_A(b) [\mathcal{N}(r) + \mathcal{N}(r')]} \\ &\times \left(\frac{\pi B_p \mathcal{N}(r) \mathcal{N}(r') T_A(b)}{1 - 2\pi B_p T_A(b) [\mathcal{N}(r) + \mathcal{N}(r')]} \right)^n. \end{aligned} \quad (13)$$

Note that Eqs. (1) and (2) have enabled us to write the leading contributions as proportional to the (Gaussian) proton-impact-parameter profile, which can then be Fourier transformed analytically. Giving up either of these approximations would force us to numerically Fourier transform the ‘‘lumpy’’ b dependence corresponding to a fixed configuration of the nucleon positions. This would make the numerical calculation much more demanding and is left for future work.

The terms with $n \geq 2$ correspond to scattering off a system of several overlapping nucleons simultaneously, leading to slower suppression with $|t|$. In practice we have verified numerically that they do not contribute to our results at the values of t we are interested in (the $n = 2$ contribution is typically $\lesssim 2\%$ of the $n = 1$ one, only reaching 5% at $-t \gtrsim 0.5 \text{ GeV}^2$), and we will neglect them in the following. This leaves us with the expression

$$\begin{aligned} |\mathcal{A}_{q\bar{q}}|^2(x_{\mathbb{P}}, r, r', \mathbf{\Delta}_T) &= 16\pi B_p A \int d^2\mathbf{b}_T e^{-B_p \Delta_T^2} e^{-2\pi B_p A T_A(b) [\mathcal{N}(r) + \mathcal{N}(r')]} \\ &\times \left(\frac{\pi B_p \mathcal{N}(r) \mathcal{N}(r') T_A(b)}{1 - 2\pi B_p T_A(b) [\mathcal{N}(r) + \mathcal{N}(r')]} \right). \end{aligned} \quad (14)$$

Equation (14) has a very clear interpretation. The squared amplitude is proportional to A times the squared amplitude for scattering off a proton, corresponding to the dipole scattering independently off the nucleons in a nucleus. This sum of independent scatterings is then multiplied by a nuclear attenuation factor

$$\begin{aligned} &\frac{e^{-2\pi B_p A T_A(b) [\mathcal{N}(r) + \mathcal{N}(r')]} }{1 - 2\pi B_p T_A(b) [\mathcal{N}(r) + \mathcal{N}(r')]} \\ &\approx e^{-2\pi(A-1) B_p T_A(b) [\mathcal{N}(r) + \mathcal{N}(r')]}, \end{aligned} \quad (15)$$

which accounts for the requirement that the dipole must *not* scatter inelastically off the other $A - 1$ nucleons in the target (otherwise the interaction would not be diffractive). Note that the factor $4\pi B_p \mathcal{N}(r, x_{\mathbb{P}}) = \sigma_{\text{dip}}^p(r, x_{\mathbb{P}})$ is the proton-dipole cross section for a dipole of size r . Thus this attenuation corresponds to the probability of a dipole with a cross section that is the average of dipoles with r and r' to pass through the nucleus. A similar expression can be found, e.g., in Ref. [11].

For comparison, the coherent cross section in our approximation is given by

$$\frac{d\sigma^{\gamma^*A \rightarrow V A^*}}{dt} = \frac{R_g^2(1 + \beta^2)}{16\pi} |\langle \mathcal{A}(x_{\mathbb{P}}, Q^2, \mathbf{\Delta}_T) \rangle_N|^2, \quad (16)$$

where in the large A and smooth nucleus limit the amplitude is

$$\begin{aligned} &\langle \mathcal{A}(x_{\mathbb{P}}, Q^2, \mathbf{\Delta}_T) \rangle_N \\ &= \int \frac{dz}{4\pi} d^2\mathbf{r}_T d^2\mathbf{r}'_T e^{-i\mathbf{b}_T \cdot \mathbf{\Delta}_T} [\Psi_V^* \Psi](r, Q^2, z) \\ &\times [1 - \exp\{-2\pi B_p A T_A(b) \mathcal{N}(r, x_{\mathbb{P}})\}]. \end{aligned} \quad (17)$$

IV. RESULTS AND DISCUSSION

We first test our dipole cross-section parametrizations and vector-meson wave functions by comparing them to HERA results [28] on diffractive J/Ψ production that is known to be well described by dipole model fits [23,32]. The comparison is quite satisfactory, as can be seen from Fig. 2. In addition to the factorized approximation [Eq. (5), ‘‘factorized IPSat’’ in Fig. 2] that we are using in the rest of this paper, also shown is the result with the original IPSat parametrization [Eq. (3), denoted ‘‘IPSat’’ in Fig. 2]. The factorized approximation differs from the original one slightly at small Q^2 , but the difference is not significant for our purpose of establishing a reasonable baseline for computing nuclear effects.

We note here that the diffractive slope parameters in the parametrizations are different, $B_p = 4.0 \text{ GeV}^{-2}$ for IPSat and

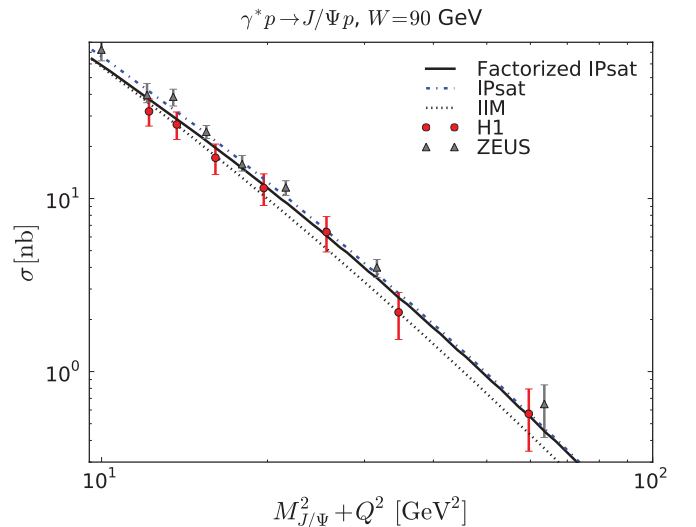


FIG. 2. (Color online) Comparison of the used dipole cross sections to HERA data [28] on diffractive vector-meson production.

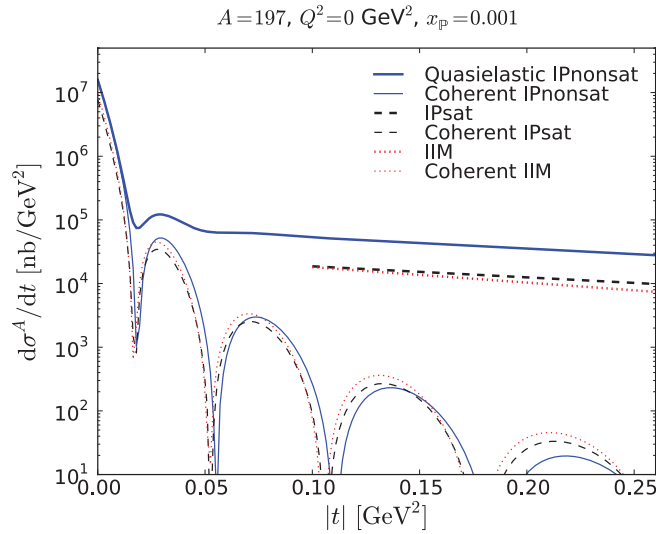


FIG. 3. (Color online) The quasielastic and coherent diffractive J/Ψ cross sections in gold nuclei at $Q^2 = 0$ and $x_{\mathbb{P}} = 0.001$. Shown are the IPsat and IIM parametrizations. We also show the result for the linearized “IPnonsat” version (used, e.g., in Ref. [4]), where the incoherent cross section is explicitly A times that of the proton. Our approximation (13) is not valid for small $|t|$; the corresponding part of the distribution has been left out.

$B_p = 5.59 \text{ GeV}^{-2}$ for IIM; since these are correlated with the other parameters in the fits leading to the parameter values used, we do not wish to alter them here. Our approximation of a factorized b dependence with a constant B does not allow us to describe the observed weak energy and Q^2 dependence of the diffractive slope. The larger B that we use for IIM comes from the σ_0 normalization in a fit to inclusive F_2 data and also agrees with the observed slopes in inclusive diffraction at large β and small $x_{\mathbb{P}}$ [33] and exclusive ρ and ϕ data [34]. The HERA J/Ψ data, on the other hand, have a smaller slope $\sim 4 \text{ GeV}^{-2}$ [28]. The t slope in the IPsat parametrization is mostly determined by this J/Ψ measurement, and an agreement with the larger measured slopes for ρ and ϕ is obtained by taking into account the larger size of the wave functions of these lighter mesons.

The differential cross section $d\sigma^{\gamma^*A \rightarrow J/\Psi A}/dt$ for $A = 197$ (gold) as a function of t is presented in Fig. 3. We show the cross section at $x_{\mathbb{P}} = 0.001$ for photoproduction. As we performed the nuclear wave-function average leading to Eq. (13) in the approximation where $|t|$ is large, neglecting the coherent contribution, we cannot extend our incoherent curves to small $|t|$. For comparison we show the corresponding “IPnonsat” result where the IPsat model is linearized in $r^2 F(x, r)$. This curve corresponds to the calculation done in Ref. [4], including both the coherent and incoherent contributions, but without the effect of multiple scattering off different nucleons (i.e., the incoherent cross section is explicitly A times the one for a proton). As one can see, the nuclear modification due to multiple scattering [resulting mostly from the factor $e^{-2\pi B_p A T_A(b)[N(r)+N(r')}]$ in Eq. (13)] is very large. In the full black disk limit of $N(r) = 1$ this factor becomes $\approx e^{-0.5A^{1/3}}$ and completely suppresses the contribution from the center of a large nucleus, leaving only an area of $\approx 2\pi dR_A \sim A^{1/3}$

contributing to the integral over \mathbf{b}_T . Thus the cross section in the black disk limit behaves as $\sim A^{1/3}$ compared to $\sim A$ in the dilute limit, so a large suppression is to be expected.

We also show in Fig. 3 the coherent cross sections [using Eq. (17)]. They are also suppressed compared to the linearized version (IPnonsat) but not by as much as the incoherent one. In the linearized version (as can be seen explicitly in Ref. [4] where this case was considered) the ratio between the coherent cross section at $t = 0$ and the incoherent one extrapolated to $t = 0$ is A . In the IPsat model we get 270 (250) and in the IIM model 300 (270) at $Q^2 = 0$ ($Q^2 = 10 \text{ GeV}^2$). This would make it slightly easier to measure the first diffractive dip in the coherent cross section since the background from the incoherent process is smaller by a factor of 2 than the linearized estimate [4].

To demonstrate the nuclear dependence further we show in Fig. 4 the ratio of the cross section in a gold nucleus to that in a nucleon as a function of Q^2 . Historically, this ratio is known as the “nuclear transparency.” Its smallness at low energy, similar to corresponding quantities in hadron-nucleus scattering, is due to the interactions of the J/Ψ as it propagates through the nucleus. The growth of the transparency toward 1 for increasing Q^2 [6,7] is a demonstration of *color transparency* (see, e.g., Refs. [8–12,35]), namely, that at large Q^2 the interacting components of the photon wave function are of smaller size r and interact weakly. In our framework color transparency is automatically present in the fact that the dipole cross section approaches zero for $r \rightarrow 0$. In Fig. 4 we also show the result (labeled “IPsat, nonsatp”) of using a nonsaturated dipole-nucleon cross section in Eq. (13). This corresponds to including unitarity effects at the nucleus level but not for a single nucleon. The observed nuclear suppression in this unphysical scenario is significantly larger than for the saturated full IPsat parametrization, showing the sensitivity of

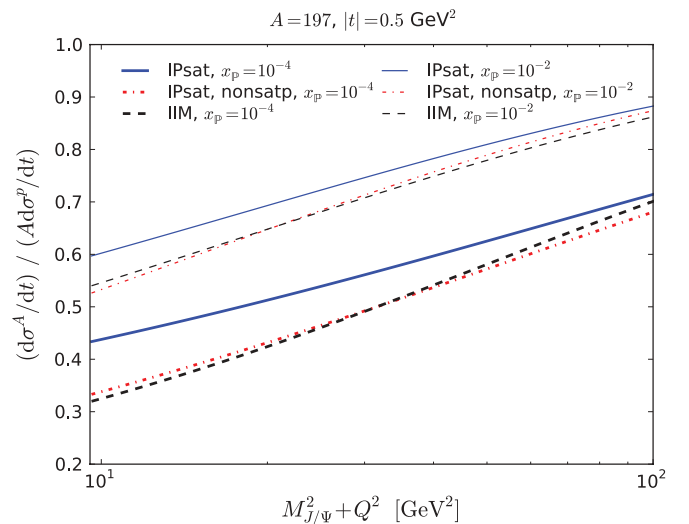


FIG. 4. (Color online) The “nuclear transparency” ratio of cross sections vs Q^2 for IPsat and IIM parametrizations at $x_{\mathbb{P}} = 10^{-2}$ (blue solid line in the top set of curves) and 10^{-4} (black dashed line in the bottom set of curves). For comparison we also include the result if unitarization effects are included at the nucleus but not at the nucleon level in the IPsat parametrization. (See text for discussion.)

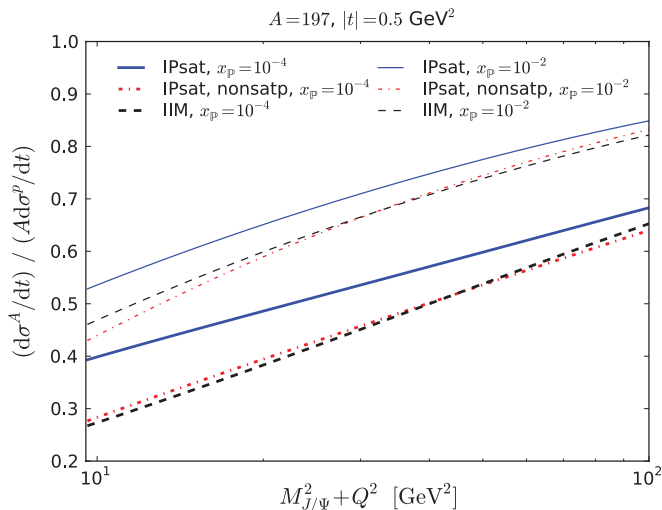


FIG. 5. (Color online) The “nuclear transparency” ratio of cross sections vs Q^2 using the gaus-LC vector-meson wave functions. The labeling is the same as in Fig. 4.

the nuclear transparency to saturation effects already at the proton level.

The IIM parametrization has a much larger nuclear suppression in incoherent diffraction, with the nuclear transparency ratio close to that of an unsaturated dipole-proton cross section. To put this in perspective recall that both parametrizations gave an equally good description of the elastic cross section measured at HERA (Fig. 2). Since IIM does this with a larger B_p than IPsat, we can infer that the typical \mathcal{N} is smaller, so that the elastic cross section $\sigma^{\text{el}} \sim B_p \mathcal{N}^2$ is of the same order. The nuclear transparency ratio, on the other hand, depends on the total dipole-nucleon cross section $\sim B_p \mathcal{N} \sim \sigma^{\text{el}}/\mathcal{N}$, which is thus larger for IIM. Thus we have a situation where both parametrizations have been fitted to inclusive F_2 data² and reproduce well the HERA J/ψ cross section but differ in their result for incoherent diffraction in nuclei. This stresses the importance of performing a global analysis of both inclusive and diffractive data to constrain the dipole cross sections and demonstrates the utility of eventual incoherent diffractive measurements in such an analysis.

Figure 5 shows the same Q^2 dependence using the gaus-LC wave function. It puts more weight on large dipole sizes, leading to a stronger nuclear suppression. The cross section ratio typically decreases by ~ 0.04 from the “boosted Gaussian” wave function, but the relative structure between the different dipole cross sections stays the same. The difference between the cross sections themselves is larger, but much of it cancels in the ratio. The existing HERA data are not precise enough to fully discriminate between different models for the vector-meson wave function, a situation that should also improve with planned new DIS experiments.

The energy dependence of the nuclear suppression (again for $A = 197$) is shown in Fig. 6 for both IPsat and IIM parametrizations at $Q^2 = 0$ and $Q^2 = 10 \text{ GeV}^2$. Again we

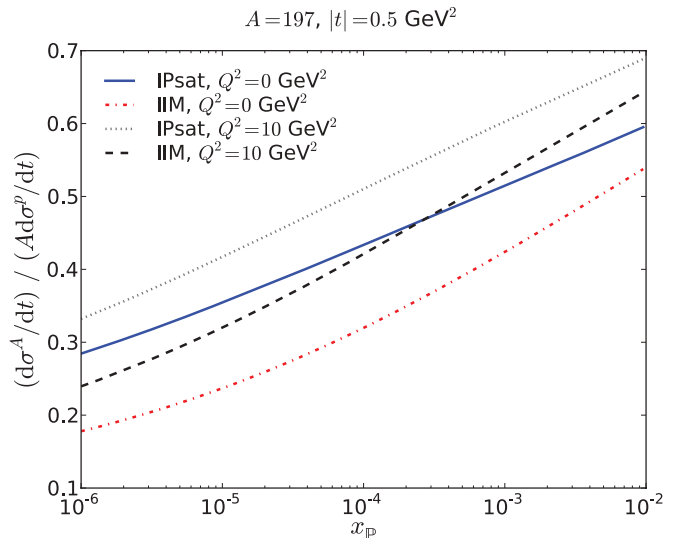


FIG. 6. (Color online) The “nuclear transparency” ratio of cross sections vs $x_{\mathbb{P}}$ using the IPsat and IIM parametrizations for $Q^2 = 0$ and $Q^2 = 10 \text{ GeV}^2$.

see the larger nuclear suppression in the IIM model than in IPsat. The differences in the energy (i.e., $x_{\mathbb{P}}$) dependence of the two dipole cross sections are more clearly visible in the photoproduction result. This is natural since in the IPsat model the energy dependence at the initial scale of the DGLAP evolution (probed at smaller Q^2) is almost flat, in stark contrast to the typical behavior resulting from BK evolution. At higher Q^2 the difference in the x dependence is smaller, although there the IPsat model, driven by the DGLAP evolution, turns over to a *faster* energy dependence. We have not extrapolated our curves to higher energies since there is no prospect of experimental measurements. One does, however, see from Fig. 6 that the curves continue to go down when extrapolated

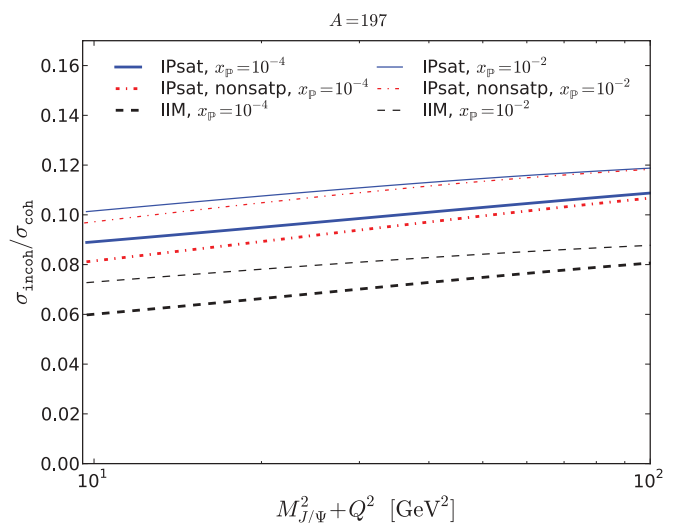


FIG. 7. (Color online) The incoherent cross section integrated over the interval $0.1 \text{ GeV}^2 < -t < 0.3 \text{ GeV}^2$ divided by the coherent cross section integrated over $0 < -t < 0.1 \text{ GeV}^2$ as a function of $Q^2 + M_{J/\psi}^2$.

²However, we have here approximated the original IPsat parametrization by factorizing the b dependence.

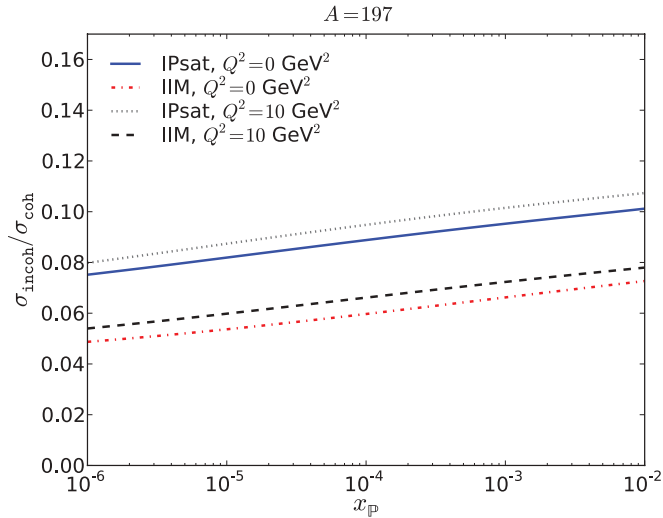


FIG. 8. (Color online) The incoherent cross section integrated over the interval $0.1 \text{ GeV}^2 < -t < 0.3 \text{ GeV}^2$ divided by the coherent cross section integrated over $0 < -t < 0.1 \text{ GeV}^2$ as a function of $x_{\mathbb{P}}$.

to smaller $x_{\mathbb{P}}$. This is to be expected since, as discussed previously, one has not yet reached the black disk limit.

In a realistic experimental setup it might be possible to detect or veto the nuclear breakup even when the momentum transfer t is not measured very accurately. In this case it will be interesting to understand how the relative magnitudes of the incoherent and coherent cross sections behave as a function of Q^2 and $x_{\mathbb{P}}$. Generally, when approaching the black disk limit, the coherent cross section increases and the incoherent one decreases. The relative change shows, however, a smaller dependence on Q^2 and $x_{\mathbb{P}}$ than the nucleus-nucleon cross-section ratio. This is shown in our parametrization in Figs. 7 and 8, where we plot the the incoherent cross section integrated over the interval $0.1 \text{ GeV}^2 < -t < 0.3 \text{ GeV}^2$ divided by the coherent cross section integrated over $0 < -t < 0.1 \text{ GeV}^2$ as a function of $Q^2 + M_{J/\psi}^2$ and $x_{\mathbb{P}}$. Figure 9 further demonstrates the relative similarity of the nuclear suppression in the coherent and incoherent cross sections. Shown is the A dependence of the ratios $(d\sigma_{\text{incoh}}^A/dt)/(A d\sigma^P/dt)$ (which, in our approximation, is independent of t) and $(d\sigma_{\text{coh}}^A/dt)/(A^2 d\sigma^P/dt)|_{t=0}$ for $Q^2 = 10 \text{ GeV}^2$ and $x_{\mathbb{P}} = 0.001$. Note that the coherent and the incoherent cross sections are normalized by different powers of A and that the width of the coherent peak at small t also depends on A .

Figures 3 and 4 are our main result. Our calculation uses as input only well-tested parametrizations that have been fit to

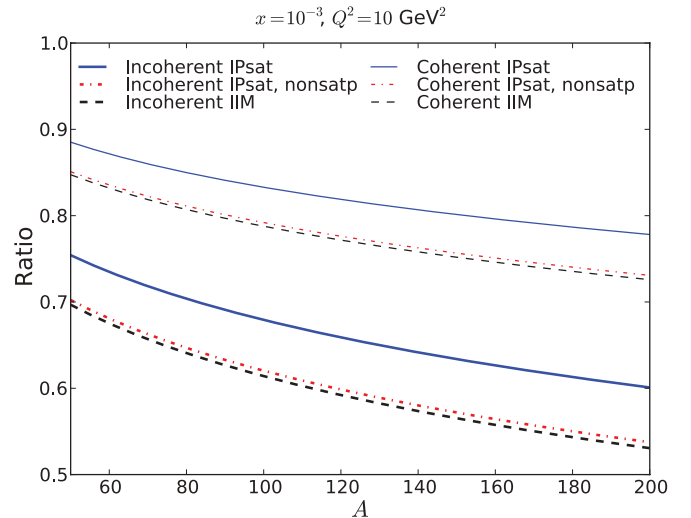


FIG. 9. (Color online) The ratio of the coherent (at $t = 0$) and incoherent (at $t = -0.5 \text{ GeV}^2$, but in our approximation this does not depend on t) cross sections to the corresponding ones for a proton, normalized with A^2 and A respectively. The ratios are plotted as a function of A for $x_{\mathbb{P}} = 0.001$ and $Q^2 = 10 \text{ GeV}^2$.

existing HERA data and nuclear geometry. We work strictly in the small x limit, which makes our formalism simple and transparent. This paper provides realistic estimates for the absolute cross sections that could be measured in future nuclear DIS experiments. We have, however, made several simplifying assumptions in our calculation, the most important being (a) the factorized impact parameter dependence, Eq. (2), (b) the assumption of independent scattering off different nucleons, Eq. (1), and (c) neglecting nucleon-nucleon correlations. Including these effects in a physically correct manner and discussing how they could be studied experimentally is left for future work. As can be seen from the values of the nuclear suppression in Figs. 4 and 6, the effects of high densities, gluon saturation, and unitarity on the incoherent cross section are large. Thus incoherent diffraction in future nuclear DIS experiments will be a sensitive probe of small- x physics.

ACKNOWLEDGMENTS

We thank E. Aschenauer, H. Kowalski, and W. Horowitz for discussions and K. J. Eskola for a careful reading of the manuscript. The work of T.L. has been supported by the Academy of Finland, project 126604. T.L. wishes to thank the INT at the University of Washington for its hospitality during the completion of this work.

- [1] A. Deshpande, R. Milner, R. Venugopalan, and W. Vogelsang, *Annu. Rev. Nucl. Part. Sci.* **55**, 165 (2005).
- [2] J. B. Dainton, M. Klein, P. Newman, E. Perez, and F. Willeke, *J. Instrum.* **1**, P10001 (2006).
- [3] M. L. Good and W. D. Walker, *Phys. Rev.* **120**, 1857 (1960).
- [4] A. Caldwell and H. Kowalski, *Phys. Rev. C* **81**, 025203 (2010).

- [5] M. L. Miller, K. Reygers, S. J. Sanders, and P. Steinberg, *Annu. Rev. Nucl. Part. Sci.* **57**, 205 (2007); B. Alver and G. Roland, *Phys. Rev. C* **81**, 054905 (2010).
- [6] M. R. Adams *et al.* (E665 Collaboration), *Phys. Rev. Lett.* **74**, 1525 (1995).
- [7] M. Arneodo *et al.* (NMC Collaboration), *Phys. Lett. B* **332**, 195 (1994); *Nucl. Phys. B* **429**, 503 (1994).
- [8] L. L. Frankfurt and M. I. Strikman, *Phys. Lett. B* **382**, 6 (1996).

- [9] L. Frankfurt, G. A. Miller, and M. Strikman, *Phys. Lett. B* **304**, 1 (1993).
- [10] S. J. Brodsky, L. Frankfurt, J. F. Gunion, A. H. Mueller, and M. Strikman, *Phys. Rev. D* **50**, 3134 (1994).
- [11] B. Z. Kopeliovich, J. Nemchik, A. Schafer, and A. V. Tarasov, *Phys. Rev. C* **65**, 035201 (2002).
- [12] L. Frankfurt, M. Strikman, and C. Weiss, *Annu. Rev. Nucl. Part. Sci.* **55**, 403 (2005).
- [13] B. Z. Kopeliovich and B. G. Zakharov, *Phys. Rev. D* **44**, 3466 (1991).
- [14] H. Kowalski, T. Lappi, and R. Venugopalan, *Phys. Rev. Lett.* **100**, 022303 (2008).
- [15] H. Kowalski, T. Lappi, C. Marquet, and R. Venugopalan, *Phys. Rev. C* **78**, 045201 (2008).
- [16] V. P. Goncalves, M. S. Kugeratski, M. V. T. Machado, and F. S. Navarra, *Phys. Rev. C* **80**, 025202 (2009).
- [17] K. Tuchin, *Phys. Rev. C* **79**, 055206 (2009).
- [18] E. Iancu, K. Itakura, and S. Munier, *Phys. Lett. B* **590**, 199 (2004).
- [19] I. Balitsky, *Nucl. Phys. B* **463**, 99 (1996); Y. V. Kovchegov, *Phys. Rev. D* **60**, 034008 (1999); **61**, 074018 (2000).
- [20] G. Soyez, *Phys. Lett. B* **655**, 32 (2007).
- [21] C. Marquet, *Phys. Rev. D* **76**, 094017 (2007).
- [22] H. Kowalski and D. Teaney, *Phys. Rev. D* **68**, 114005 (2003).
- [23] H. Kowalski, L. Motyka, and G. Watt, *Phys. Rev. D* **74**, 074016 (2006).
- [24] L. D. McLerran and R. Venugopalan, *Phys. Rev. D* **49**, 2233 (1994).
- [25] K. J. Golec-Biernat and A. M. Stasto, *Nucl. Phys. B* **668**, 345 (2003).
- [26] J. Jalilian-Marian and Y. V. Kovchegov, *Prog. Part. Nucl. Phys.* **56**, 104 (2006).
- [27] J. Bartels, K. Golec-Biernat, and H. Kowalski, *Phys. Rev. D* **66**, 014001 (2002).
- [28] S. Chekanov *et al.* (ZEUS Collaboration), *Nucl. Phys. B* **695**, 3 (2004); A. Aktas *et al.* (H1 Collaboration), *Eur. Phys. J. C* **46**, 585 (2006).
- [29] A. G. Shuvaev, K. J. Golec-Biernat, A. D. Martin, and M. G. Ryskin, *Phys. Rev. D* **60**, 014015 (1999); A. D. Martin, M. G. Ryskin, and T. Teubner, *ibid.* **62**, 014022 (2000).
- [30] G. Watt and H. Kowalski, *Phys. Rev. D* **78**, 014016 (2008).
- [31] M. Alvioli, H. J. Drescher, and M. Strikman, *Phys. Lett. B* **680**, 225 (2009).
- [32] C. Marquet, R. Peschanski, and G. Soyez, *Phys. Rev. D* **76**, 034011 (2007).
- [33] S. Chekanov *et al.* (ZEUS Collaboration), *Eur. Phys. J. C* **38**, 43 (2004); A. Aktas *et al.* (H1 Collaboration), *ibid.* **48**, 749 (2006).
- [34] C. Adloff *et al.*, *Eur. Phys. J. C* **13**, 371 (2000); S. Chekanov *et al.* (ZEUS Collaboration), *Nucl. Phys. B* **718**, 3 (2005).
- [35] G. A. Miller and M. Strikman, *Phys. Rev. C* **82**, 025205 (2010).